

# Crystal structure and spectroscopic properties of 4-acetaminopyridine and its protonated form

Bojidarka B. Koleva<sup>1\*</sup>, Rositsa Nikolova<sup>2</sup>, Atanas Tchapanov<sup>3</sup>, Tsonko Kolev<sup>5</sup>, Heike Mayer-Figge<sup>1</sup>, Michael Spitteler<sup>4</sup>, William S. Sheldrick<sup>1</sup>

<sup>1</sup>*Lehrstuhl für Analytische Chemie, Ruhr-Universität Bochum, Universitätsstraße 150, 44780 Bochum, Germany.*

<sup>2</sup>*University of Sofia "St. Kl. Ohridsky", Department of Organic Chemistry, Sofia 1164, Bulgaria*

<sup>3</sup>*South-West University, Department of Chemistry, Blagoevgrad 1341, Bulgaria*

<sup>4</sup>*Institut für Umweltforschung, Universität Dortmund, Otto-Hahn-Strasse 6, 44221 Dortmund, Germany*

\* Corresponding author: e-mail: BKoleva@chem.uni-sofia.bg

4-Acetaminopyridine dihydrate and its protonated form, stabilized as the hydrochloride salt have been synthesized and spectroscopic elucidated in solution and in the solid-state by means of the linear-polarized solid state IR-spectroscopy (IR-LD), UV-spectroscopy, TGA, DSC, and the positive and negative ESI MS. Quantum chemical calculations were used to obtain the electronic structure, vibrational data and the electronic spectra. The spectroscopic and theoretical data are compared with the structure of the first compound obtained by single crystal X-ray diffraction. The effect of N<sub>py</sub> protonation on the optical and magnetic properties of a 4-acetaminopyridine is discussed.

**Keywords:** 4-Acetaminopyridine, protonated form, crystal structure, solid-state linear polarized IR-spectroscopy, UV-spectroscopy, quantum chemical calculations, <sup>1</sup>H- and <sup>13</sup>C NMR, ESI MS, TGA and DSC.

## INTRODUCTION

Aminopyridines are biologically active compounds. They act by an inhibition of the voltage-dependent K<sup>+</sup>-channels<sup>1–3</sup>, due to their ability to facilitate nerve transmission. Aminopyridines have been applied to reverse anaesthesia and muscle relaxation<sup>4</sup> and have been proposed as drugs for the treatment of multiple sclerosis<sup>5</sup>, myasthenia gravis<sup>6</sup>, spinal cord injuries<sup>7</sup>, botulism<sup>8</sup> and Alzheimer's disease<sup>9</sup>. Aminopyridines are weak bases that can exist in either the neutral or the cationic protonated form at physiological pH. This characteristic complicates the elucidation of the mechanism and the site of action<sup>10,11</sup>. On the other hand, the amides of the aminopyridines have been intensively studied in the co-crystallization processes that are currently receiving considerable attention, partly because of fundamental interest in molecular-recognition driven assembly procedures. As part of our systematic study of pyridine derivatives and their protonated forms<sup>12–17</sup>, we now present a spectroscopic and structural study of 4-acetaminopyridine dihydrate (**1**) and its N<sub>py</sub> protonated form (**2**), both in the solution and in the solid state using the methods of single crystal X-ray diffraction, <sup>1</sup>H- and <sup>13</sup>C-NMR, positive and negative ESI mass spectrometry, UV-spectroscopy, conventional and linear polarized IR-spectroscopy, and the TGA and DSC analysis. Quantum chemical calculations at the DFT, MP2 and CIS levels of theory and the 6-311++G\*\* basis set are employed for predicting and supporting the experimentally observed optical properties.

Despite the fact that aminopyridinium derivatives have been widely investigated in the past only three crystal structures of 4-acetaminopyridine, bis(acetato-O)-bis(4-(N-acetyl-amino)pyridine)-aqua-copper(II)<sup>18</sup>, bis(hydrogen fluoride) dihydrate bis(4-acetaminopyridine) decandioic acid<sup>19</sup> and 4-acetaminopyridinium hydroglutamate<sup>19</sup>. We now reported the crystal structure of 4-acetaminopyridine dihydrate (**1**).

## EXPERIMENTAL

### Methods

The X-ray diffraction intensities were measured in the  $\omega$  scan mode on a Siemens P4 diffractometer equipped with Mo K $_{\alpha}$  radiation ( $\lambda = 0.71073 \text{ \AA}$ ,  $\theta_{\max} = 25^{\circ}$ ) and the structure was solved by direct methods and refined against F<sup>2</sup><sup>20,21</sup>. An ORTEP plot illustrates the anion and cation structures at the 50% probability level. Relevant crystallographic structure data and refinement details are presented in Table 1, the selected bond distances and angles in Table 2. The hydrogen atoms were constrained to calculated positions and refined using riding models in all the cases.

Conventional and polarized IR-spectra were measured on a Thermo Nicolet OMNIC FTIR-spectrometer (4000 – 400 cm<sup>-1</sup>, 2 cm<sup>-1</sup> resolution, 200 scans) equipped with a Specac wire-grid polarizer. The non-polarized solid-state IR spectra were recorded using the KBr disk technique. The oriented samples were obtained as a colloid suspension in a nematic liquid crystal ZLI 1695. The theoretical approach and the experimental technique for preparing the samples as well as the procedures for the polarized IR-spectra interpretation and the validation of this new linear-dichroic infrared (IR-LD) orientation solid-state method for accuracy and precision have been previously presented<sup>22–25</sup>. The influence of the liquid crystal medium on the peak positions and the integral absorbances of the guest molecule bands, the rheological model, the nature and balance of the forces in the nematic liquid crystal suspension system, and the morphology of the suspended particles have also been discussed<sup>22–25</sup>.

The positive and negative ESI mass spectra were recorded on a Fisons VG Autospec instrument employing 3-nitrobenzylalcohol (Sigma-Aldrich) as the matrix.

Ultraviolet (UV-) spectra were recorded on Tecan Safire Absorbance/Fluorescence XFluor 4 V 4.40 spectrophotometer operating between 190 and 900 nm, using the

**Table 1.** Crystal and refinement data for 4-acetaminopyridine dihydrate

Empirical formula	C <sub>7</sub> H <sub>9</sub> N <sub>2</sub> O
Formula weight	137.16
Temperature (K)	293(2)
Wavelength (Å)	0.71073
Crystal system, space group	Monoclinic, P2 <sub>1</sub> /n
Unit cell dimensions	<i>a</i> = 12.015(2) Å
	<i>b</i> = 9.860(2) Å
	<i>c</i> = 14.270(3) Å
	β = 105.68(3) °
Volume (Å <sup>3</sup> )	1627.6(6)
Z	9
Calculated density (Mg · m <sup>-3</sup> )	1.259
Absorption coefficient (mm <sup>-1</sup> )	0.087
F(000)	657
Crystal size (mm)	0.37 x. 0.30 x 0.21
θ range for data collection	1.97 ≤ θ ≤ 27.51
Limiting indices	-1 ≤ <i>h</i> ≤ 15, -1 ≤ <i>k</i> ≤ 12, -18 ≤ <i>l</i> ≤ 18
Reflections collected / unique	4874 / 3719, R(int) = 0.0252
Absorption correction	ψ scans
Goodness-of-fit on F <sup>2</sup>	1.000
Final R indices [I > 2σ(I)]	R1 = 0.0833, wR2 = 0.1748
R indices (all data)	R1 = 0.2123, wR2 = 0.2326

**Table 2.** Selected experimental bond lengths [Å] and angles [°] for 4-acetaminopyridine dihydrate from crystallographic data

N4 C234 1.366(5)	N2 C3 1.368(5)
N4 C235 1.408(5)	N2 C6 1.413(4)
C236 C8 1.385(5)	N1 C1 1.336(5)
C236 C235 1.396(5)	N1 C4 1.342(5)
C235 C233 1.398(5)	C7 C4 1.389(5)
O4 C234 1.231(4)	C7 C6 1.406(5)
C234 C10 1.510(5)	C6 C55 1.394(5)
C233 C9 1.379(5)	O3 C3 1.242(4)
N3 C9 1.348(5)	C55 C1 1.392(5)
N3 C8 1.348(5)	C3 C2 1.502(5)
C234 N4 C235 128.5(3)	C3 N2 C6 128.4(3)
C8 C236 C235 118.7(4)	C1 N1 C4 115.2(4)
C236 C235 C233 117.4(4)	C4 C7 C6 119.2(4)
C236 C235 N4 124.6(4)	C55 C6 C7 117.2(4)
C233 C235 N4 118.0(3)	C55 C6 N2 125.6(3)
O4 C234 N4 122.6(4)	C7 C6 N2 117.2(3)
O4 C234 C10 122.2(4)	C1 C55 C6 118.3(4)
N4 C234 C10 115.1(3)	N1 C4 C7 124.4(4)
C9 C233 C235 119.6(4)	O3 C3 N2 122.8(4)
C9 N3 C8 115.7(4)	O3 C3 C2 122.2(4)
N3 C9 C233 124.0(4)	N2 C3 C2 115.0(3)
N3 C8 C236 124.6(4)	N1 C1 C55 125.7(4)

solvents water, methanol, dichloromethane, tetrahydrofurane, acetonitrile, acetone, 2-propanol and ethyl acetate (all Uvasol, Merck products) at a concentration of  $2.5 \cdot 10^{-5}$  M in 0.0921 cm quartz cells.

*Quantum chemical calculations* were performed with GAUSSIAN 98 program packages<sup>26</sup>. The output files are visualized by means of the ChemCraft program<sup>27</sup>. The geometries of the compounds were optimized at two levels of theory: second-order Moller-Pleset perturbation theory (MP2) and density functional theory (DFT) using the 6-311++G\*\* basis set. The DFT method employed is B3LYP, which combines Becke's three-parameter non-local exchange function with the correlation function of Lee, Yang and Parr. The molecular geometry was fully optimized by the force gradient method using Bernys'

algorithm. For every structure the stationary points found on the molecule potential energy hypersurfaces were characterized using the standard analytical harmonic vibrational analysis. The absence of the imaginary frequencies, as well as of negative eigenvalues of the second-derivative matrix, confirmed that the stationary points correspond to the minima of the potential energy hypersurfaces. The vibrational frequencies and infrared intensities were checked to establish which kind of performed calculations agree best with the experimental data. In our cases, the DFT method provides more accurate vibrational data, as far as the calculated standard deviations of respectively 11 cm<sup>-1</sup> (B3LYP) and 18 cm<sup>-1</sup> (MP2) corresponding to groups, which do not participate in intra- or intermolecular hydrogen bonds, are concerned. So, the B3LYP/6-311++G\*\* data are presented for above discussed modes, where a modification of the results using the empirical scaling factor 0.9614 is made to achieve better correspondence between the experimental and theoretical values. The UV spectra in the gas phase and in ethanol solution were obtained by CIS/6-311++G\*\* and TDDFT calculations.

## Synthesis

4-Acetaminopyridine dihydrate (**1**) was obtained in the following way: 4.0 g (0.042 mol) of 4-aminopyridine (Sigma Aldrich products) were mixed with 5.6 (0.55 mol) (CH<sub>3</sub>CO)<sub>2</sub>O with a continuous stirring at 100°C for 1h. After that 50 ml H<sub>2</sub>O was added and the stirring continued for 0.5h. 80 ml 30% NaOH in water were added to the neutralization of the reaction product and generate CH<sub>3</sub>COOH. The extraction of the final product was achieved with CH<sub>2</sub>Cl<sub>2</sub>. Suitable single crystals for X-ray diffraction were obtained after recrystallisation from a solvent mixture ethanol:water (1:1). The compound (**2**) was obtained by dissolving 0.4521 g of (**1**) in 10 ml water and adding of 1 ml c. HCl. After a week the resulting white precipitate was filtered off, washed with water and dried under air at 298 K.

## RESULTS AND DISCUSSION

### Crystallographic data of 4-Acetaminopyridine dihydrate (1)

The asymmetric unit of 4-acetaminopyridine dihydrate, is depicted in Fig. 1. The compound crystallizes in the centrosymmetric space group  $P2_1/n$  and contains two independent. The molecules of 4-acetaminopyridine are connected by moderate intermolecular hydrogen bonds to the co-crystallized water molecules in the structure, ( $\text{NH}\cdots\text{OH}_2$  (2.901, 2.883 Å),  $\text{HOH}\cdots\text{O}=\text{C}$  (2.832, 2.819 Å) and  $\text{HOH}\cdots\text{Npy}$  (2.830, 2.855 Å), thus forming infinite layers (Fig. 2) at the stacking distance of 3.504 Å. The amide fragments exhibit a trans-configuration and are effectively planar with dihedral angle values of  $177.3(6)^\circ$  and  $179.7(8)^\circ$ , respectively.

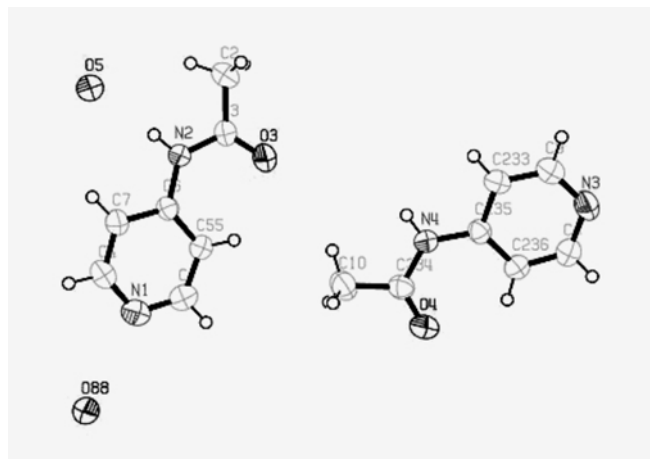


**Figure 1.** The structure of 4-acetaminopyridine dihydrate (1), showing the atom-labeling scheme in the independent molecules. Displacement ellipsoids are drawn at the 50% probability level

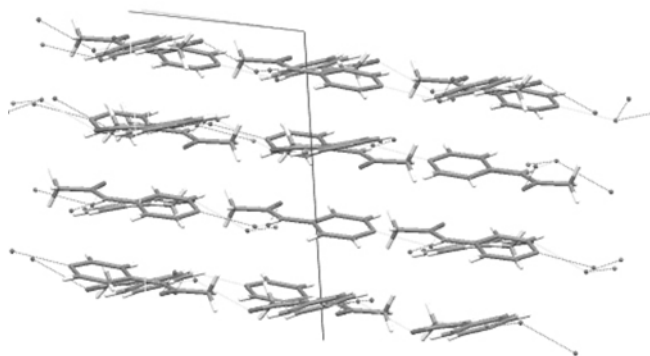
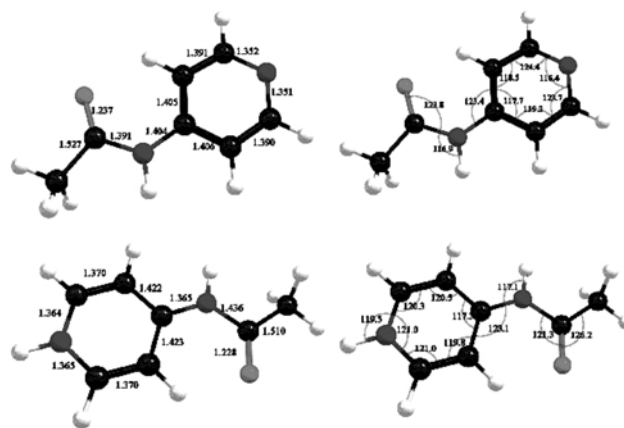


**Figure 2.** Hydrogen bonding in 4-acetaminopyridine dihydrate (1)

### Theoretical calculations

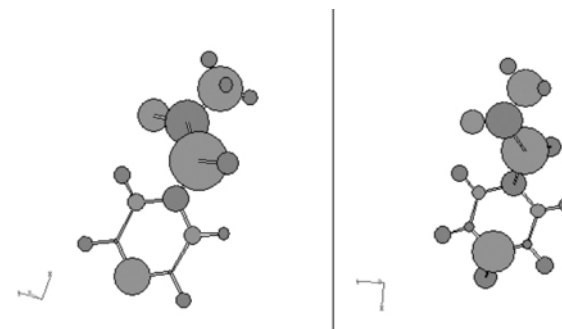
The theoretical conformational analysis of the neutral and protonated form of 4-acetaminopyridine confirms the stabilization of trans-configuration of the amide fragment with  $E_{\text{rel}}$  values of 0.0 kJ/mol (1) and 0.1 kJ/mol (2) (Scheme 1), respectively. The dihedral  $\text{HN}-\text{C}=\text{O}$  angle of  $179.9(9)^\circ$  in both cases correlates well with the X-ray structure for the neutral form. Bond lengths and angles are summarized in Scheme 1 and also indicate a good agreements between the theoretical approximation method and the experimental crystallographic data. Differences of

less than 0.0216 Å and  $2.4(1)^\circ$  are observed (compare Table 2 and Scheme1).



**Scheme 1.** Optimized geometry parameters

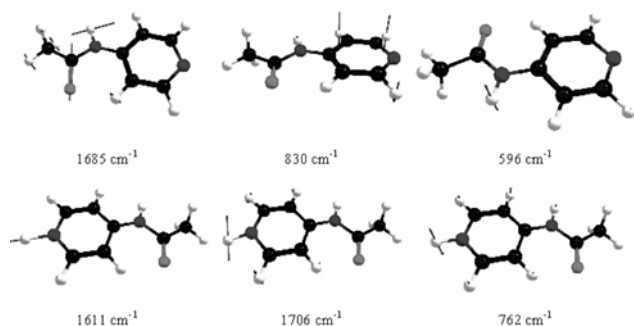
In contrast to the  $\text{N}_{\text{py}}$  protonated forms of 4-aminopyridine<sup>14</sup> and 4-dimethylaminopyridine<sup>17</sup>, where the  $\text{N}_{\text{py}}$  protonation leads to a distortion of the aromatic character of the pyridine ring and stabilization of the quinoid-like form, this process has no significant affect on the aromaticity of the skeleton of 4-acetaminopyridine. An illustration of this charge distribution of both forms (Scheme 2) shows that the  $\text{N}_{\text{py}}$  protonation leads to a difference of 0.065 eV the  $\delta^+$  charge of the  $\text{N}_{\text{py}}$  nitrogen.



**Scheme 2.** Chemical diagram of the single charge electron density distribution

Additional confirmation of this finding follows from the theoretical IR-spectra (Fig.3), where the main differences between (1) and (2) are connected with the presence of the protonated  $\text{N}^+\text{H}$  group in the second case leading to corresponding characteristic stretching and bending vibrations (Scheme 3). The  $\nu_{\text{N}^+\text{H}}$  vibration is obtained at a lower frequency than that of  $\text{nNH}$  ( $3488\text{ cm}^{-1}$  and  $3383\text{ cm}^{-1}$ ). In contrast, the bending  $\delta_{\text{N}^+\text{H}}$  band shifted to a higher frequency ( $1571\text{ cm}^{-1}$ ) than the corresponding band of  $\text{dNH}$  (Amide II,  $1471\text{ cm}^{-1}$ ). The in-plane (i.p.) and out-of-plane (o.p.) modes of the pyridine fragments are practically unaffected by the  $\text{N}_{\text{py}}$  protonation. The  $\nu_{\text{C}=\text{O}}$  (Amide I) band is obtained at about  $1685\text{ cm}^{-1}$  in the neutral form and at about  $1706\text{ cm}^{-1}$  in the corresponding protonated form. The  $\nu_{\text{NH}}$  stretching vibration in the neutral form is observed at  $3398\text{ cm}^{-1}$  which represents a shift of  $90\text{ cm}^{-1}$  to lower frequency in comparison to protonated form. We can conclude that the amidation of 4-aminopyridine hinders the formation of the quinoid-like form, that is typical of the  $\text{N}_{\text{py}}$  protonated salts 4-

aminopyridine and 4-dimethylaminopyridine<sup>14, 17</sup>. Additional confirmation follows from the calculated low frequency shifting of the pyridine o.p. mode from 830 cm<sup>-1</sup> in the neutral form to 762 cm<sup>-1</sup> in the protonated one (Scheme 3), which can be described as a monosubstituted aromatic fragment.



**Scheme 3.** Visualization of selected transition moments in (1) and (2)

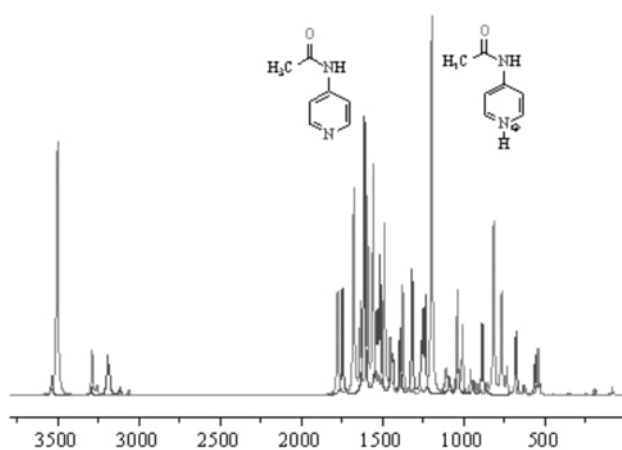


**Figure 3.** Theoretical IR spectra of the neutral and protonated forms of 4-acetaminopyridine

#### Conventional and linear-polarized IR-spectra

The theoretical conclusions were confirmed experimentally by investigating the conventional and linear polarized IR-spectra of (1) and (2) (Fig. 4). The  $\nu_{\text{NH}}$  stretching vibration is observed at 3440 cm<sup>-1</sup> in (1), while the band is shifted at lower frequency to 3423 cm<sup>-1</sup> in (2). The  $\nu_{\text{N+H}}$  vibration is observed as a relatively broad band at 3469 cm<sup>-1</sup> in the spectrum in Fig. 4.2. The amide I modes are observed as strong intensive bands at 1687 cm<sup>-1</sup> (1) and 1675 cm<sup>-1</sup> (2), respectively. The intensive band at 1712 cm<sup>-1</sup> in Fig. 4.2 can be assigned to  $\delta_{\text{N+H}}$  and exhibits a typical value for a protonated N<sup>+</sup>H group in the pyridines<sup>12-17</sup>. The intensive o.p. bands of (1) and (2) are at 833 cm<sup>-1</sup> and 763 cm<sup>-1</sup>, correlating well with the theoretically predicted values (see above). The  $\gamma_{\text{NH}}$  deformation vibrations are observed as broad bands at 636 cm<sup>-1</sup> (1) and 598 cm<sup>-1</sup> (2), respectively.

The elimination of the amide I band in both compounds leads to the disappearance of the IR-band of the corresponding  $\nu_{\text{NH}}$  stretching vibration (Fig.4.3), indicating the trans-configuration of the amide fragments, the state of affairs that was theoretically predicted for both compounds and experimentally confirmed by single crystal X-ray diffraction of (1). In the case of (1) the procedure leads to the observation of second pairs of maxima with the same origin, due to the presence of two independent molecules of 4-acetaminopyridine (Figs. 4.3 and 1) in the unit cell.

#### UV-spectra

The UV-spectra of the compounds (1) and (2) are depicted in Fig. 5. A comparison with the data of the salt of the monoprotonated 4-aminopyridine as well as that of 4-dimethylaminopyridine and 3,4-dimethylaminopyridine salts<sup>14-16</sup> show that compound (1) is characterized by two maxima at 240 nm ( $\pi \rightarrow \pi^*$ ,  $\epsilon$  12341 l.mol<sup>-1</sup>.cm<sup>-1</sup>) and 260 nm (B-band,  $\epsilon$  = 1167 l.mol<sup>-1</sup>.cm<sup>-1</sup>), in contrast to the

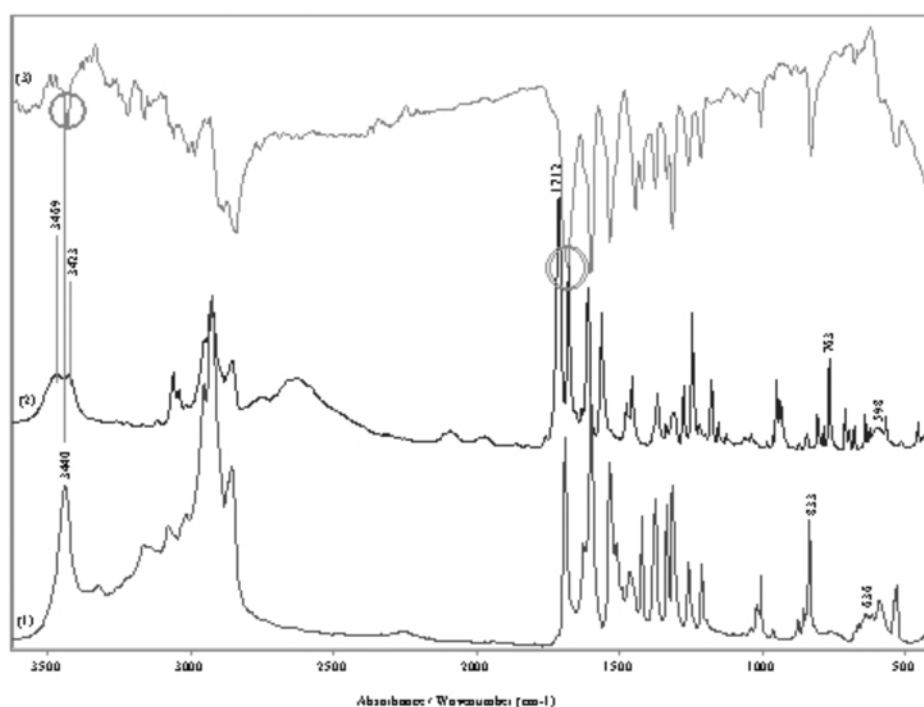


**Figure 4.** Non-polarized IR spectra of 4-acetaminopyridine dihydrate (1) and its protonated form (2) and reduced IR-LD spectrum of (1) after elimination of the band at 3440 cm<sup>-1</sup> (3)

mentioned pyridinium derivatives where only the first band is typical. The  $N_{py}$  protonation leads only to a weak bathochromic effect for the first maximum (4 nm) as well as the hypochromic one ( $\epsilon$  2351 l.mol<sup>-1</sup>.cm<sup>-1</sup>). These results give future support to an assumption about the retention of aromatic character in (1) following of  $N_{py}$  protonation. Moreover, our theoretical calculations for (2) in aqueous solution give bands at 245 nm and 266 nm with  $E = 4.72$  and  $3.21$  eV and  $f = 0.2934$  and  $0.3421$ , respectively

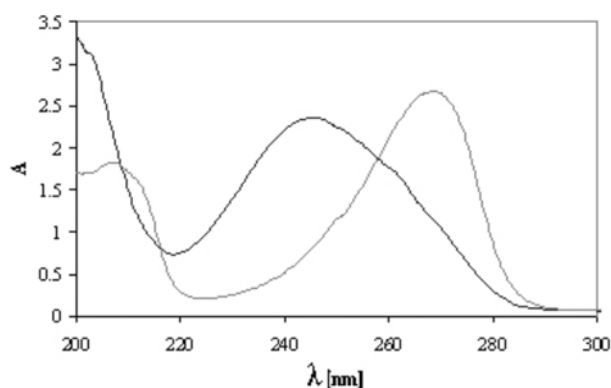


**Figure 5.** UV-spectra of neutral (black) and protonated form (grey) in solution

#### <sup>1</sup>H and <sup>13</sup>C-NMR data in solution

The <sup>1</sup>H-NMR spectrum of (1) exhibits chemical shift differences  $\Delta\delta$  for the signals of the aromatic protons in the range 7.83 – 7.96 ppm of 0.04 ppm (H2, H3), 0.05 ppm (H5) and 0.13 ppm (H6) in comparison to the corresponding data for (2), which unambiguously confirms the conclusion that  $N_{py}$  protonation leads to the retention of the aromatic character. This protonation also has practically no effect on the <sup>13</sup>C-NMR chemical signals and  $\Delta\delta$  values of less than 0.1 ppm are observed. These results are similar to those obtained for other pyridinium derivatives, where the aromatic and quinoid-like form have been characterized spectroscopically<sup>14–17</sup>.

#### CONCLUSION

We have reported on the spectroscopic and structural elucidation of 4-acetaminopyridine dihydrate and its protonated form, stabilized as the hydrochloride, by means of single crystal X-ray diffraction, linear-polarized solid state IR-spectroscopy (IR-LD), UV-spectroscopy, TGA, DSC, and positive and negative ESI MS. Quantum chemical calculations were used to obtain the electronic structure, vibrational data and electronic spectra. The first compound crystallizes in the centrosymmetric space group  $P2_1/n$  and contains two nonequivalent molecules, connected by moderate intermolecular,  $NH\cdots OH_2$  (2.901, 2.883 Å),  $HOH\cdots O=C$  (2.832, 2.819 Å) and  $HOH\cdots N_{py}$  (2.830, 2.855 Å), hydrogen bonds, leading to the formation of infinite layers. The amide fragment is *trans*-configured with dihedral angle values of 177.3(6)° and 179.7(8)°, respectively. The comparison of the optical and magnetic properties of (1) and (2) both in solution and in the solid state, shows that in contrast to the monoprotonated salts of 4-aminopyridine, 4-dimethylaminopyridide or 3,4-diaminopyridine, where the

quinoid-like form or partial aromatic distortion of pyridine have been observed<sup>14–17</sup>. The  $N_{py}$  protonation of 4-acetaminopyridine has practically no significant influence on the spectroscopic properties of the aromatic pyridine fragment.

#### Acknowledgements

B.K. wishes to thank the Alexander von Humboldt Foundation for a Fellowship and T.K. the DAAD for the grant within the priority program "Stability Pact South-Eastern Europe" and the Alexander von Humboldt Foundation

#### Supporting information

Crystallographic data for the structural analysis have been deposited with the Cambridge Crystallographic Data Centre, CCDC 697434. Copies of this information may be obtained from the Director, CCDC, 12 Union Road, Cambridge, CB2 1EZ, UK (Fax: +44 1223 336 033; e-mail: deposit@ccdc.cam.ac.uk or <http://www.ccdc.cam.ac.uk>).

#### LITERATURE CITED

1. Molgo, J., Lemeignan, M., Peradejordi, F. & Lechat, P. (1985). Presynaptic effects of aminopyridines on the neuromuscular junction of vertebrates *J. Pharmacol. (Paris)* 16, 109 – 121.
2. Kirsch, G.E., Yeh, J.Z. & Oxford, G.S. (1986). Modulation of aminopyridine block of potassium currents in squid axon, *Biophys. J.* 50, 637 – 644.
3. Molgo, J., Lemeignan, M., Lechat, P. & Peradejordi, F. (1985). Increase in evoked transmitter release from motor nerve terminals by some amino N-heterocyclic compounds I. Comparative experimental activities and extracellular pH-dependence, *Eur. J. Med. Chem.* 20, 149 – 153.
4. Carlsson, C., Rosen, I. & Nilsson, E. (1993) Can 4-Aminopyridine be Used to Reverse Anaesthesia and Muscle Relaxation? *Acta Anaesthesiol. Scand.*, 27, 87 – 90.
5. Schwid, S., Petrie, M., McDermott, M., Tierney, D., Maso, D. & Goodman, A. (1997). Quantitative assessment of sustained-release 4-aminopyridine for symptomatic treatment of multiple sclerosis, *Neurology* 48, 817 – 821.
6. McEvoy, K.M., Windebank, A.J., Daube, J.R. & Low, P.A., (1989). 3,4-Diaminopyridine in the treatment of Lambert-Eaton myasthenic syndrome. *New Engl. J. Med.* 321, 1567 – 1571.
7. Segal, J.L. & Brunnemann, S.R. (1997). 4-Aminopyridine improves pulmonary function in quadriplegic humans with long-standing spinal cord injury. *Pharmacotherapy* 17, 415 – 423.
8. Sellin, L.C. (1981). The action of botulinum toxin at the neuromuscular junction. *Med. Biol.* 59, 11 – 20.
9. Davidson, M., Zemishlany, J.H. & Mohs, R.C. (1988). Alzheimer's Disease: A Report of Progress in Research. *Biol. Psychiatry* 23, 485 – 490.
10. Meves, H. & Pichon, H. (1979). The effects of 4-aminopyridine on the potassium current in internally perfused giant axons of the squid. *J. Physiol. Lond.* 251, 60 – 63.
11. Raust, J., Goulay-Dufay, S., Le Hoang, M., Pradeau, D. & Guyon, F. (2007). Stability studies of ionised and non-ionised 3,4-diaminopyridine: Hypothesis of degradation pathways and chemical structure of degradation products, *J. Pharmaceut. Biomed. Anal.* 43, 83 – 88.
12. Ivanova, B. & Mayer-Figge, H. (2005). Crystal structure and Solid state IR-LD spectral analysis of new mononuclear Cu(II) complex with 4-aminopyridine. *J. Coord. Chem.* 58, 653 – 659.

13. Ivanova, B., Arnaudov, M. & Mayer-Figge, H. Molecular spectral analysis and crystal structure of 4-aminopyridinium tetrachloropalladate(II) complex salt. (2005). *Polyhedron* 24(13), 1624 – 1630.
14. Koleva, B., Trendafilova, E., Arnaudov, M., Sheldrick, W.S. & Mayer-Figge, H. (2006). Structural analysis of a mononuclear copper(II) complex of 3-aminopyridine. *Trans. Met. Chem.* 31, 866 – 873.
15. Koleva, B.B., Kolev, T., Tsanev, T., Kotov, St., Mayer-Figge, H., Seidel, R.W. & Sheldrick, W.S. (2008). Spectroscopic and structural elucidation of 3,4-diaminopyridine and its hydrogentartarate salt. Crystal structure of 3,4-diaminopyridinium hydrogentartarate dehydrate. *J. Mol. Struct.* 881, 146 – 155.
16. Koleva, B.B., Kolev, T., Tsanev, T., Kotov, St., Mayer-Figge, H., Seidel, R.S. & Sheldrick, W.S. (2008). 3,4-diaminopyridine bis(perchlorate): structural and spectroscopic elucidation? *Struct. Chem.* 19(1), 13 – 20.
17. Koleva, B.B., Kolev, T., Seidel, R.W., Tsanev, T., Mayer-Figge, H., Spitteller, M. & Sheldrick, W.S. (2008). Spectroscopic and structural elucidation of 4-dimethylaminopyridine and its hydrogensquarate. *Spectrochim. Acta, Part A*, 71., 695 – 702.
18. Emsley, J., Arif, M., Bates, P. & Hursthouse, M. (1988). Bis(acetato)bis[4-(N-acetylamino)pyridine]aquacopper(II)-hydrogen fluoride-hydrate (1/2/2): X-ray structure reveals H<sub>2</sub>O·HF hydrogen bonded in the lattice. *J. Chem. Soc. Dalton. Trans.* 1493 – 1497.
19. Aakeroy, C.B., Hussain, I., Forbes, S. & Desper, J. (2007). Exploring the hydrogen-bond preference of N-H moieties in co-crystals assembled via O-H(acid) N(py) intermolecular interactions. *Cryst. Eng. Comm.* 9, 46 – 55.
20. Sheldrick, G.M. 1995, SHELXTL, Release 5.03 for Siemens R3 crystallographic research system. Siemens Analytical X-Ray Instruments, Inc., Madison, USA.
21. Sheldrick, G.M. 1997, SHELXS97 and SHELXL97. University of Göttingen, Germany.
22. Ivanova, B.B., Arnaudov, M.G. & Bontchev, P.R. (2004). Linear-dichroic infrared spectral analysis of Cu(I)-homocysteine complex. *Spectrochim Acta* 60(4)A, 855 – 862.
23. Ivanova, B.B.; Tsalev, D.L. & Arnaudov, M.G. (2006). Validation of reducing-difference procedure for the interpretation of non-polarized infrared spectra of *n*-component solid mixtures. *Talanta* 69, 822 – 828.
24. Ivanova, B.B., Simeonov, V.D., Arnaudov, M.G. & Tsalev, D.L. (2007). Linear-dichroic infrared spectroscopy – validation and experimental design of the orientation technique as suspension in nematic liquid crystal. *Spectrochim Acta* 67A, 66 – 75.
25. Koleva, B.B., Kolev, T., Simeonov, V., Spassov, T. & Spitteller, M. (2008). Linear polarized IR-spectroscopy of partial oriented solids as a colloid suspension in nematic liquid crystal – new tool for structural elucidation of the chemical compounds. *J. Incl. Phen.* 61, 319 – 333.
26. Frisch, M.J., Trucks, G.W., Schlegel, H.B., Scuseria, G.E., Robb, M.A., Cheeseman, J.R., Zakrzewski, V.G., Montgomery, Jr.J.A., Stratmann, R.E., Burant, J.C., Dapprich, S., Millam, J.M., Daniels, A.D., Kudin, K.N., Strain, M.C., Farkas, Ö., Tomasi, J., Barone, V., Cossi, M., Cammi, R., Mennucci, B., Pomelli, C., Adamo, C., Clifford, S., Ochterski, J., Petersson, G.A., Ayala, P.Y., Cui, Q., Morokuma, K., Salvador, P., Dannenberg, J.J., Malick, D.K., Rabuck, A.D., Raghavachari, K., Foresman, J.B., Cioslowski, J., Ortiz, J.V., Baboul, A.G., Stefanov, B.B., Liu, G., Liashenko, A., Piskorz, P., Komáromi, I., Gomperts, R., Martin, R.L., Fox, D.J., Keith, T., Al-Laham, M.A., Peng, C.Y., Nanayakkara, A., Challacombe, M., Gill, P.M.W., Johnson, B., Chen, W., Wong, M.W., Andres, J.L., Gonzalez, C., Head-Gordon, M., Replogle, E.S. & Pople, J.A. Gaussian 98, Gaussian, Inc., Pittsburgh, PA, 1998.
27. Zhurko, G.A. & Zhurko, D.A., ChemCraft: Tool for treatment of chemical data, Lite version build 08 2005.